Light Metals 2015
Edited by: Margaret Hyland
TMS (The Minerals, Metals & Materials Society), 2015

STUDY OF THE STRUCTURE AND THERMOPHYSICAL PROPERTIES OF THE SIDE LEDGE IN HALL-HÉROULT CELLS OPERATING WITH MODIFIED BATH COMPOSITION

Sándor Poncsák[1], László Kiss[1], Alexandre Belley[1], Sébastien Guérard[2], Jean-François Bilodeau[2]
[1]Université du Québec à Chicoutimi 555, Boul. de l'Université, Chicoutimi, QC, Canada
[2]CRDA, Rio Tinto Alcan 1955 Boul. Mellon, Jonquière, QC, Canada

Keywords: Aluminum electrolysis, side ledge, structure, thermo-physical properties, modified bath composition

Abstract

Recently, there are efforts to change bath chemistry used for aluminium electrolysis, in order to decrease operation temperature, cell voltage, etc. Such modifications have a significant impact on the whole Hall-Héroult process, including the composition, the structure, and the thermal properties of the protecting side ledge. Consequently, the heat balance of the cell can be shifted and thus the optimal parameters of the cell operation can be modified. This paper presents some observations and a few results obtained with side ledge of a semi-industrial cell, operating with modified bath composition. Results show that the main components of the continuous phase in the side ledge remain the cryolithe mixed with some chiolite. However, the apparition of new compounds increases the inhomogeneity, resulting in a slight decrease of the thermal conductivity of side ledge.

Introduction

It is well known, that the molten cryolithe is the only widely used solvent for alumina. However, many different additives are used in the aluminum reduction cells in order to decrease liquidus temperature, increase electrical conductivity of the electrolyte and minimize the formation of sodium at the bath-metal interface [1]. Lately, potassium, lithium, chloride etc. ions containing bath were tested as well for aluminum electrolysis [2-10]. Those bathes have reduced liquidus temperatures, but unfortunately, significantly smaller solubility of the alumina as well.

The modification of the bath composition can alter the composition, the structure and different properties (such as liquidus, enthalpy of fusion, density, thermal conductivity, etc.) of the protecting side-ledge. The composition of the side-ledge is closer to that of the bath when the solidification takes place fast, but alters significantly, when solidification is slow [11]. As a good insulator that can change phase at least partially during cell operations, the side ledge plays an important role in the heat balance and the thermal stabilisation of the cells.

In the light of the above-mentioned facts, the knowledge of the chemical and physical properties of the side ledge (such as the distribution of chemical composition, structure, thermo-physical properties etc.) is crucial to any reliable thermal model of the aluminum reduction cells.

It is hard to find any information in open literature about the characterization of side-ledge formed from modified composition bath, because companies consider them confidential [5]. What is more, the chemical analysis by XRD becomes harder when Li^+, K^+ or Mg^{2+} ions are present in the cell [12]. Lately, the composition, structure and phase change temperatures of crust formed from K and Li containing bath were studied [13-15]. However, the crust has a different composition than that of the side-ledge.

In the frame of a cooperative research project between Rio Tinto Alcan and UQAC, side ledge samples were extracted from post-mortem semi-industrial experimental cells, operating with modified bath composition. The samples were taken shortly after the shutdown of the cell in order to carry out different chemical, image and thermo-physical analysis. In the present paper, a few results of the complete study are presented.

Experimental

Sample collection and preparation

Samples were cut from the cold side-ledge of a semi-industrial cell, operating with modified bath composition, a few days after its shutdown, using special equipment designed for this purpose. No water was used to the cooling of the sample during cutting, in order to avoid the chemical transformation of the side ledge as well as prevent toxic gas emissions. Samples were taken at different positions of the cell, namely at the middle of the positive and negative sides as well as at the corner, both at the bath and the metal levels. At certain locations, the side ledge was too fragile or too thin to be sampled.

Samples were identified (including their orientation) and put in hermetically closed barrels, filled with argon gas and containing some desiccant at the bottom in order to avoid any reaction with moisture or oxygen. Samples were used to carry out chemical and image analysis as well as dilatometric and thermal conductivity measurements.

Chemical Analysis

X-ray Diffraction (XRD) technique was used to determine chemical composition of the samples. Tests were carried out using *Panalytical X'pert* diffractometer, equipped with copper tube and fast detector (model *PIXEL*). Results were refined with the Rietveld method, optimized for the bath. As unfortunately the widely applied XRD technique can detect only crystalline phases, the LECO method was utilized additionally to obtain the total amount of alumina, including amorphous phases. The last technique uses the fact that the alumina is the only oxygen source in the bath and thus in the side-ledge. Consequently, if the sample is heated under air-free environment to very high temperatures in the presence of carbon, the quantity of the carboxyl gases produced is proportional to that of the initial alumina content. The LECO tests were carried out with LECO O836 instrument.

Samples for both XRD and LECO tests were crushed and homogenized to -100 mesh size.

Image Analysis

Scanning Electron Microscope (SEM JEOL JSM 6460 LV with Oxford SiLi detector and Inca software) was used to obtain information about both surface topography and elementary composition. When secondary electron imaging mode (SEI) is applied, the SEM permits to produce a very high-resolution image about the structure of the sample surface with a relatively large depth of field. On the other hand, in back-scattered electron mode (BSE), the SEM reveals elementary composition of very small areas.

Samples were mounted rigidly in a red sample holder resin (called specimen stub), grounded and coated by the deposition of an ultra-thin, conducting layer (gold). This can prevent accumulation of static charge and increases the signal to noise ratio. Red coloration of the holder resin allowed to validate the evaluation of the local porosity using optical images. 10 small areas by samples were chosen for porosity studies, all excluding the fissures, which were formed probably due to thermal shrinkage during the cooling-down of the cell.

Measurement of the thermal conductivity

It is important to determine thermo-physical properties at higher temperatures, in order to approach the conditions similar to those found in operating industrial cells.

The variation of the thermal conductivity of side ledge with the temperature was measured with the laser flash method [16]. It involves the illumination of a disc shaped sample at one side with a short, high-energy laser flash and the measurement of the thermal response on the opposite side. More details about this method are presented in the literature [16-17].

For this study, small disc shaped samples (∅ 12.5 mm, thickness 3mm) were prepared with rotational axes normal to the cell sidewall. The surfaces of the samples were painted black and matte in order to achieve an emissivity as high as possible, close to 1. Bigger superficial pores were filled with a paste to avoid direct penetration of illuminating light into the samples. Such modification can increase slightly the measured value of the heat conductivity [17]. However, this modification does not affect any comparative study.

The laser flash tests were carried out using a FlashLineTH 5000 (Anter Corp.) apparatus with infrared laser source and radiometric detector. The radiation thermometer determines the average temperature of the rear surface. Measurements were carried out between 100 and 500 °C under argon atmosphere. Higher temperatures were avoided for security reasons. Namely, certain AlF_3 rich particles can melt even at 700 °C [18] that might damage the apparatus, especially the temperature detector. At least 3 samples were taken from every position and measurements were repeated 5 times at all temperature plateaus.

As a first approximation, the thermal diffusivity (α) can be determined simply from the sample thickness (L) and the time necessary to reach the half of the amplitude of variation of the temperature on the rear side of the sample ($t_{1/2}$). During the measurements the Clark and Taylor correction method was used to take into account the heat losses during the tests. To obtain the thermal conductivity (k), the density (ρ) and the heat capacity (C_p) must be known at the temperature of the test:

$$k = \alpha \rho C_P \qquad \text{equation 1}$$

The density variation was followed by a dilatometer. The volumetric heat capacity ρCp can be obtained by the flash method itself, if a reference sample with known heat capacity is also used. The design of the apparatus and an identical surface coating must assure that the same amount of energy is absorbed by both the studied samples and the reference. Furthermore, their thermal conductivities must be in the same order of magnitude in order to minimize the error due to the heat loss.

Dilatometric study

The initial apparent density of the porous samples at room temperature was determined by volume and masse measurements. The thermal dilatation of rod shaped samples (100mm height with a diameter of 12.5mm) in the range of 25 – 500 °C were tested under argon atmosphere, using the UNITHERM^{TM} 1101 (Anter Corp.) dilatometer. The measurement of this property is necessary to obtain the variation of the density of the side ledge as the function of the temperature. Density data are used for the calculation of the thermal conductivity from the thermal diffusivity data obtained with the flash method.

Results and discussion

Appearance and image analysis

Examples of side-ledge samples taken at bath (left) and metal (right) levels are shown in figure 1. Similarly to earlier observations, obtained with regular bath [17] the side-ledge at metal level seems to be much more homogenous, compared to the bath level. Black zones could be observed only at the bath level. A few metal droplets were found too, but only at the metal level (figure 2).

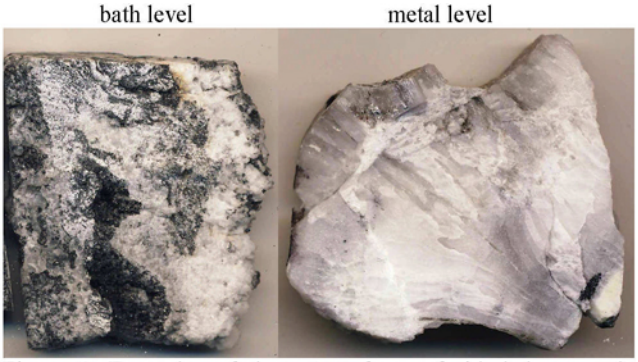

Figure 1. Examples of the cut surfaces of side-ledge samples taken at bath and metal levels

Figure 3 shows a typical example of a BSE-SEM image of the side-ledge. Despite the strong macroscopic inhomogeneities, more general tendencies can be observed. In almost all the cases, the continuous phase (big gray areas on figure R3; 9-10) is composed of either pure cryolithe or a mixture of cryolithe and AlF_3. This phase is dominating the side-ledge zones, which look to be white or gray on macroscopic view. The formation of pure cryolithe is

more probable when solidification takes place slowly, close to the equilibrium state (low heat flux) [11]. On the other hand, excess AlF_3 indicates fast freezing, where the bath was trapped into the solid phase without the possibility of mass diffusion [11].

Figure 2. Aluminum droplets enclosed in the side-ledge taken at the metal level

Small inclusions (pale discontinuous-phases on figure 3; 1-8) are containing all the elements composing the bath. Minor elements of the bath like Ca can be found only in this phase and not in the continuous matrix. Such inclusions can have amorphous or elongated shapes, depending on position and composition. Some elongated inclusions are parallel to each other, indicating locally a dominant direction of heat flux during the solidification.

BSE images reveal the presence of pores and fissures as well. The latest were formed probably during the cooling down of the cell due to thermal shrinkage.

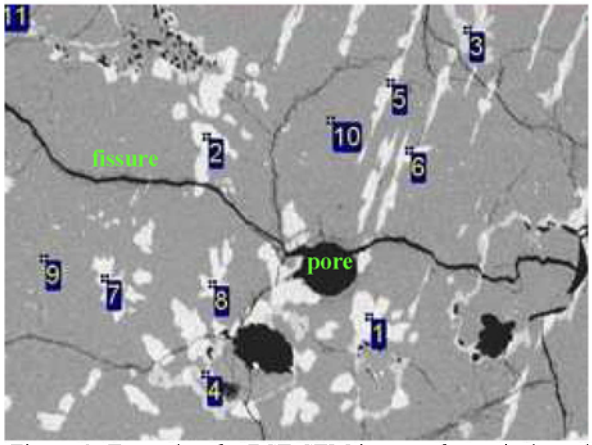

Figure 3. Example of a BSE-SEM image of a typical small zone of side-ledge sample obtained with back-scattered electron mode

The black zones in the side-ledge indicate the presence of carbon inclusions. Such particles can be found only at bath level and they are more frequent close to the sidewall. An example of their image obtained with BSE technique is shown on figure 4. Those particles are composed mainly by a carbon dominated continuous phase, enclosing a few small inclusions, containing the elements of the bath. In the most cases, the carbon is accompanied by a small amount of sulfur.

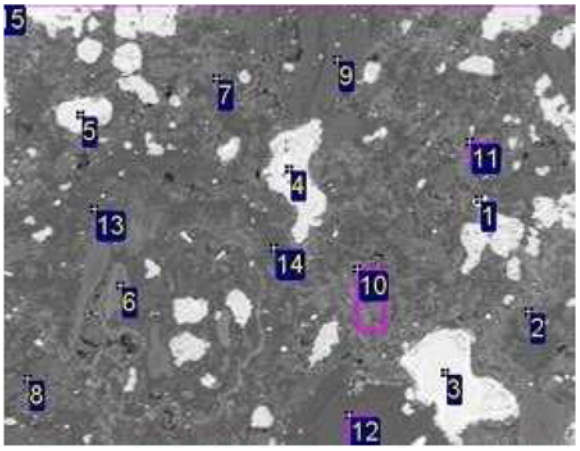

Figure 4. Example of a BSE-SEM image of small, black carbon-rich zone of side-ledge sample obtained with back-scattered electron mode

Porosity

The porosity of the side-ledge samples is very low, remains always below 10% [table 1]. Porosity seems to be slightly higher at the corner and lower on the middle of the positive side of the electrolysis cell. No significant correlation with the height (level) or distance from the sidewall could be observed.

Table I. Variation of the side-ledge porosity with the position in the electrolysis cell, obtained by analysis of SEI-SEM images

Position in the cell	Level	Local porosity		
		Minimum	Maximum	Average
Negative side	bath	0	0.7	0.2
	metal	0	4.2	0.84
Positive side	bath	0.1	4.4	1.98
Corner	bath	1.5	5.1	2.8
	metal	0.2	8.4	2.1

The impact of porosity on the apparent thermal conductivity has been studied since long time [19]. One of the basic models was developed by Maxwell and Rayleigh [19] for the case when uniform spherical pores are distributed in regular cubic array:

$$\frac{k}{k_s} = \frac{1 - P\left(1 - b * {k_g}/{k_s}\right)}{1 + P(b-1)} \qquad \text{equation 1}$$

where $b = 3k_s / (2k_s + k_g)$

k represents the apparent thermal conductivity of the porous media, k_S and k_g are the conductivities of the pure solid matrix and that of the gas filling the pores respectively, while P denotes the porosity. In spite of the initial hypothesis of the regular distribution of uniform pores, this equation gives a good approximation even for more irregular porous materials when the porosity remains under 0.5.

Figure 5 shows the variation of the dimensionless thermal conductivity with the porosity, computed with the Maxwell-Rayleigh equation, using data of air and of side-ledge with less than 0.5% of porosity for k_g and k_s respectively for air – side-ledge system. An average value of the side-ledge data measured

by laser flash method was used for k_s. Figure 5 suggests that the decrease of thermal conductivity due to the porosity cannot be greater than 14% in the side-ledge.

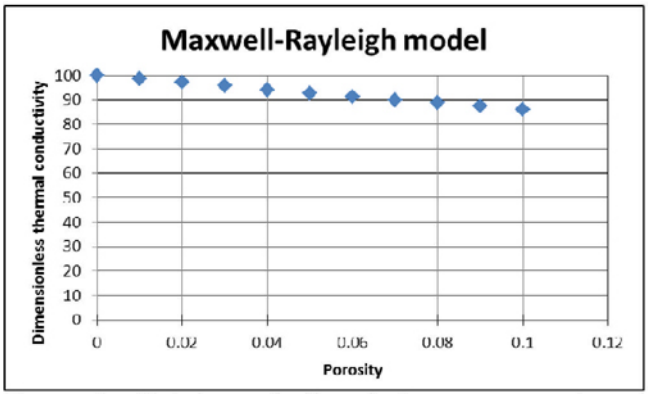

Figure 5. Variation of dimensionless apparent thermal conductivity with the porosity, computed with the Maxwell-Rayleigh model for air-side-ledge system

Chemical analysis

Global (average) molecular composition of the side-ledge samples was measured with XRD and LECO techniques. Figure 6 shows the variation of the cryolithe content with position in the electrolysis cell. The cryolithe content is the highest at the corner and lowest at the negative side, especially at the bath level. This is in according to the heat distribution in the cell. Namely, the corners are generally the coldest places in the cell as they are cooled from two directions, while the middle of the sidewall is cooled practically from one direction. What is more, observation suggests that the negative side of the cell is generally warmer compared to the positive (opposite) side. This means that the side-ledge at the corner is the most stable. On the other hand, side-ledge can change in thickness faster and more often on the negative side when anode effect, anode change, adjustment of anode height (ACD) or other heat flux affecting cell operations take place. The fast solidification results in a side-ledge composition closer to the bath composition. Consequently the cryolithe content must be lower, as the formation of cryolithe is promoted by conditions close to equilibrium.

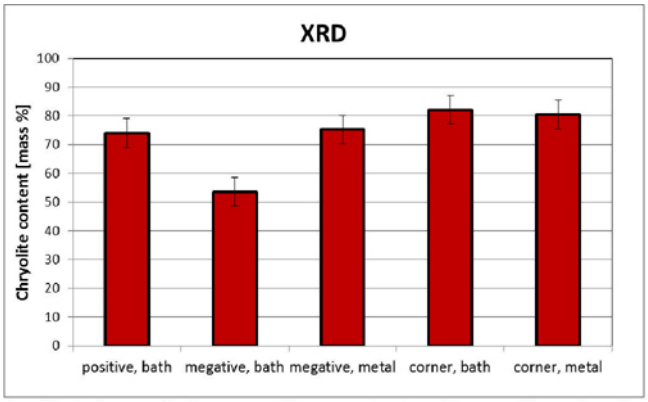

6. Variation of the cryolithe content with position in the electrolysis cell; "positive" and "negative" notes indicates the positive and negative sides of the cell respectively

Dilatometry

The variation of the density of side-ledge of modified bath samples in the temperature range of 25 – 500 °C was measured by a dilatometer. In this interval, the density decreases gradually about 5% due to thermal dilatation (figure 7). Samples taken at metal level had slightly lower density, but all the samples fell in the range that was obtained earlier for traditional bath (blue area on figure 7) [17]. Density values were used for the computation of the thermal conductivity.

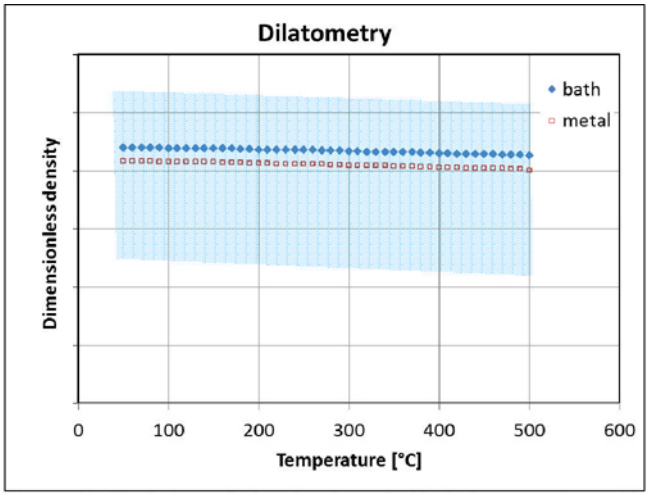

Figure 7. Variation of the density of side-ledge samples with temperature

Thermal conductivity

Dimensionless thermal conductivity data obtained with laser flash method for side-ledge formed in cell with modified bath is shown in figure 8. The conductivity seems to remain almost constant in the measured temperature range. The lack of tendency is the result of the significant increase of the heat capacity that is able to compensate the combined decreases of the density and the diffusivity. The blue-shaded zone in figure 8 indicates the range of thermal conductivity data, obtained with traditional bath side-ledge, using the same flash method [17].

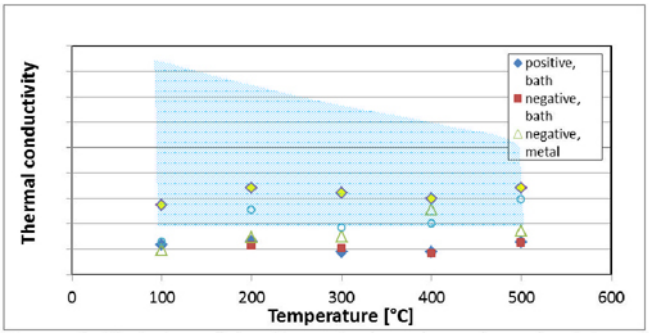

Figure 8. Variation of the dimensionless thermal conductivity of side-ledge samples with temperature

Results shows, that the side-ledge taken from the corner has the biggest conductivity, especially at the bath level. This is the area where the side-ledge is the most stable in the operating cell and which contains the biggest portion of pure cryolithe. The presence of small aluminum droplets at the metal level does not seem to

improve significantly the apparent conductivity for the whole samples. The samples taken at the bath level in the corner contain an extended dark, carbon rich area, which can contribute well to the better conduction, as it was shown earlier [17].

One can conclude that the side-ledge of the modified bath has somewhat lower conductivity, especially at low temperatures. As its porosity seems to be very low and it is composed of non-connected, closed pores, the increase of porosity cannot explain this behavior. The only possible explanation remains the bigger diversity of chemical compounds and thus a bigger number of phase limits, which can slow down the propagation of the heat.

Conclusions

Post-mortem side-ledge samples were taken a few days after the shutdown from different horizontal positions and heights in a semi-industrial cell, operating with modified bath composition. A complete analysis of those samples revealed the following tendencies:

- The side-ledge samples taken at the bath level seem to be much more inhomogeneous than those coming from the metal level. The same tendency was observed earlier with traditional bath. Only the side-ledge taken from the bath level contains dark, carbon-rich zones, while small aluminum droplets can be found solely at metal level.
- The white and grey zones are composed mainly of cryolithe or cryolithe mixed with excess AlF_3 matrix. The small inclusions in them contain all the elements of the bath; among others, all the calcium content is concentrated in those small particles. The black zones are dominated by carbon accompanied by some sulfur.
- In certain zones, the inclusions are forming parallel, elongated particles, indicating an orientation during crystallization.
- If the cracks – appeared probably during the cooling down of the cell – are neglected, the remaining porosity seems to be very low, less than 10%. What is more, the pores are not interconnected.
- The density of side-ledge samples decrease about 5% between 25 and 500 °C and it is comparable to the density of the side-ledge formed in traditional bath.
- The thermal conductivity of the side-ledge of the modified bath is lower, compared to that of traditional bath. As the porosity remains low, this can be explained by the bigger diversity of chemical compounds and thus a greater number of phase boundaries between grains.
- The thermal conductivity of the side-ledge in the corner is higher compared to the middle of the cell walls. This is the zone where the proportion of the pure cryolithe is the highest and the side-ledge is the most stable during cell operation.

Acknowledgment

The authors would like to thank *Rio Tinto Alcan* to give access to their shutdown industrial cells to take side ledge samples. This work could not be realized without the valuable financial support of *Rio Tinto Alcan* and the *National Sciences and Engineering Research Council of Canada* (NSERC). The analytical groups of ARDC, managed by Andris Innus and François Laplante are thanked as well for performing image analysis, XRD and LECO analyses respectively.

References

1. W. E. Peterson, R. E. Miller, "First Century of Aluminum Process Technology 1886-1986", John Wiley & Sons, (2013) p. 121
2. R. G. Cheney, "Potline Operation with Lithium-Modified Bath", JOM, **35**, 12 (December 1983), p. 47
3. A. Solheim et al., "Liquidus temperatures for primary crystallization of cryolithe in molten salt systems of interest for aluminum electrolysis", Metall. And Mat. Trans. B, **27**, 5 (1996) p. 739
4. E. Skybakmoe, A. Solheim and A. Sterten, "Alumina Solubility in Molten Salt Systems of Interest for Aluminum Electrolysis and Related Phase Diagram Data", Metall. And Mat. Trans. B, **28**, 1 (2007) p. 81
5. H. Kvande, "Bath Cemistry and Aluminum Cell Performance – Facts, fictions and doubts", JOM, **46**, 11 (Nov. 1994), p. 22
6. Y. Zaikov et al., "Electrolysis of Aluminum in the Low Melting Electrolytes Based on Potassium Cryolite", *TMS Light Metals 2008*, p. 505
7. E. Frazer and J. Thonstad, "Alumina Solubility and Diffusion Coefficient of the Dissolved Alumina Species in Low-Temperature Fluoride Electrolytes", Metall. And Mat. Trans. B, **41B**, (2010) p. 543
8. J Hives and J Thonstad, "Electrical Conductivity of Low-Melting Electrolytes for Aluminum Smelting", Electrochimica Acta, **49**, 28, (2004) p. 5111
9. P. Fellner, J. Hivek and J Thonstad, "Transport Numbers in the Molten System NaF-KF-AlF_3-Al_2O_3", *TMS Light Metals 2011*, p 513
10. National Research Council (U.S.). Materials Advisory Board, "Processes for Extracting Alumina from Nonbauxite Ores", NMAB 278 (December 1970)
11. A. Solheim and L.I.R. Staen, "On the Composition of Solid Deposits Frozen out from the Cryolitic Melts", *TMS Light Metals 1997*, p 325
12. N. I. Thahyono et al. "Improving XRD Analysis for Complex Bath Chemistries – Investigation and Challenges Faced", *TMS Light Metals 2014*, p. 573
13. W. Haupin " Defining Bath Ratio in the Presence of LiF and MgF_2", *TMS Light Metals 1996*, p. 219
14. A. T. Tabereaux, T. R. Alcorn, L. Tremblay, "Lithium Modified Low Ratio Electrolyte Chemistry for Improved Performance in Modern Reduction Cells", *TMS Light Metals 1993*, p. 221
15. Q Zhang et al. "Composition and Thermal Analysis of Crust Formed from Industrial Anode Cover", *TMS Light Metals 2013*, p. 675
16. W.J. Parker, R.J. Jenkins, C.P. Butler, G.L. Abbott, "Flash Method of Determining Thermal Diffusivity, Heat Capacity, and Thermal Conductivity", *J Appl. Phys.* **32**, 9 (1961) p. 1679
17. S. Poncsák, L. Kiss, R. St-Pierre, S. Guérard, and J. Bilodeau, "Structural Characterisation and Thermophysical Properties of the Side Ledge in Hall-Héroult Cells", *TMS Light Metals 2013*, p. 585
18. D.J. Walker and T.A. Utigard, "Alumina Agglomerates in Aluminum Smelters", *TMS Light Metals 1995*, p. 425
19. W. Woodside, "Calculation of the Thermal Conductivity of Porous Media", Canadian Journal of Physics, **36**, 7, (1958) p. 815